Novel Low-Complexity Graph-Based Turbo Equalization for Single-Carrier and Multi-Carrier FTN Signaling

Tianhang Yu[1], Minjian Zhao[2*], Jie Zhong[3], Jian Zhang[4] and Pei Xiao[5]

Abstract

We propose a novel turbo detection scheme based on the factor graph serial-schedule belief propagation equalization algorithm with low complexity for single-carrier faster-than-Nyquist (FTN) and multi-carrier FTN signaling. In this work, the additive white Gaussian noise channel and multi-path fading channels are both considered. The iterative factor graph-based equalization algorithm can deal with severe intersymbol interference and intercarrier interference introduced by the generation of single-carrier and multi-carrier FTN signals, as well as the effect of multi-path fading. With the application of Gaussian approximation, the complexity of the proposed equalization algorithm is significantly reduced. In the turbo detection, Low density parity check code is employed. The simulation results demonstrate that the factor graph-based turbo detection method can achieve satisfactory performance with low complexity.

Index Terms

SC-FTN, MC-FTN, FG-SS-BP equalization, GA, low complexity, multi-path fading channel

T. Yu, M. Zhao (corresponding auther), J. Zhong and J. Zhang are with the College of Information Science and Electronic Engineering, Zhejiang University, Hangzhou 310027, China (E-mail: [1] tianhang0318@zju.edu.cn; [2*] mjzhao@zju.edu.cn; [3] zhongjie@zju.edu.cn; [4] zjfly2008@zju.edu.cn). P. Xiao is with the Institute for Communications Systems Home of 5G Innovation Centre, University of Surrey, Guildford, Surrey, GU2 7XH, United Kingdom (E-mail: [5] p.xiao@surrey.ac.uk).

This work was supported by the National Science Foundation of China (NSFC) under Grant 91538103, and the National High Technology Research and Development Program (863 Program) of China under Grant 2014AA01A707.

Part of the manuscript was presented at the IEEE Vehicular Technology Conference-Spring, May 2016, Nanjing, China.

I. Introduction

Recently, Long-Term Evolution (LTE), also known as 4G, has been widely rolled out in many countries. There is no doubt that 4G can accommodate the rapid increase of user data rate and system capacity to some extend. However, the demand of higher capacity is still growing dramatically. In the past few years, the concept of faster-than-Nyquist (FTN) has been proposed as a means to increase the efficiency for 5G mobile communications. The single-carrier FTN (SC-FTN) traces back to the 1970s [1]. However, it was hardly acceptable due to the impractical complexity at that time. With the development of the new silicon technology and the urgent requirement for "faster" transmission, SC-FTN has drawn more and more attention [2]. It offers an alternative to more efficient transmission by packing up to 25% more data in the same bandwidth at the same energy per bit, without loss of the minimum Euclidean distance in the signaling space [1]. Nevertheless, the intersymbol interference (ISI) is unavoidable, which leads to the increase of the receiver complexity [3]. Hence, the design of an SC-FTN detector performing close to the optimal detector of an orthogonal system with low complexity is necessary.

Up to now, a number of equlization algorithms have been developed for SC-FTN signaling. The optimal way of dealing with the ISI is the maximum-likelihood sequence estimation (MLSE), which can be implemented with a standard Viterbi algorithm (VA) [4]. However, the complexity of the standard VA is too high. In order to reduce the complexity, a truncated modified VA (TMVA) has been proposed in [5] and a soft-output TMVA (SOTMVA) combined with a residual ISI canceller (RISIC) in [5] is developed to improve the performance. Another scheme based on the M-algorithm BCJR (M-BCJR) has been proposed in [6]. Although these reduced-complexity algorithms are suboptimal, their complexity remains high, especially for systems employing high order constellations.

All of the above equalization algorithms only consider the SC-FTN systems under the additive white Gaussian noise (AWGN) channel. Among the latest ones, a low-complexity frequency-domain equalization (FDE) receiver structure is proposed in [7] and multi-path scenarios are also considered. Despite the low complexity, the performance of FDE is not satisfactory. Moreover, the insertion of the cyclic prefix (CP) also reduces the system efficiency. Motivated by the limitations of performance and the benefits of low complexity, a three-stage-concatenated SC-FTN signaling transceiver based on FDE is proposed in [8]. However, the complexity is increased due to the three-stage structure, and the efficiency reduction caused by CP is still a drawback of the proposed transceiver.

In order to provide further improvements, FTN concept has been extended in some ways, e.g. to multi-carrier systems. The earliest research dealing with multi-carrier FTN (MC-FTN) signaling is documented in [9], and since then a number of papers about MC-FTN signaling have been published [10] [11] [12]. Such systems can also be called spectrally efficient frequency division multiplexing (SEFDM) [13]. As the name implies, it is in a manner similar to orthogonal frequency division multiplexing (OFDM), while violating the orthogonality principle by employing closely packed subcarriers to save bandwidth [15]. However, the advantages of the MC-FTN signaling are achieved at the cost of a more complex receiver dealing with the intrinsic intercarrier interference (ICI).

In [13], an inverse fractional Fourier transform (IFrFT) algorithm is employed for the generation of MC-FTN signals. This algorithm needs a bank of modulators running at the subcarrier frequencies, which is impractical when the number of subcarriers is large. Worse sitll, this system is more sensitive to frequency offsets and timing errors. In [16], a simple framework for the generation of MC-FTN signals based on the inverse discrete Fourier transform (IDFT) is proposed. This framework can be implemented efficiently using inverse fast Fourier transform (IFFT), which leads to a low complexity similar to the implementation complexity of OFDM [17].

Several papers focusing on the detection algorithms of the MC-FTN signaling have been reported in the literature. A BCJR-based detector is proposed in [9]. Since the optimal detection is overly complex due to the ICI, an alternative detection mechanism based on generalized sphere decoding (GSD) is proposed in [13]. Then, a novel hybrid soft iterative detection (ID) algorithm together with fixed sphere decoding (FSD) is proposed in [14]. Unfortunately, this detector is merely suitable for small size systems. In order to reduce the complexity further, a multi-band architecture for a large non-orthogonal system is proposed in [18]. However, only the simulation results under the AWGN channel have been presented.

In this work, a low-complexity detection scheme based on the factor graph serial-schedule belief propagation (FG-SS-BP) equalization algorithm is proposed. We have proposed the graph-based equalization algorithm for BPSK-modulated SC-FTN systems under the AWGN channel in [19]. The contributions of this paper can be summarized as follows. (1) This is the first extension of the proposed algorithm to SC-FTN systems with high order modulation, such as multiple phase shift keying (MPSK) and multiple quadrature amplitude modulation (MQAM) under the AWGN channel and multi-path fading channels. (2) The factor graph (FG) of MC-FTN signaling has never been presented before this paper and we extend the FG-SS-BP algorithm to MC-FTN systems under the AWGN channel as well as multi-path fading channels. (3) A novel continuous phase CP insertion scheme is proposed in MC-FTN systems for the first time.

The remainder of this paper is organized as follows. Section II introduces the SC-FTN system model, as well as the FG-SS-BP equalization algorithm under the AWGN channel and multi-path fading channels.

In Section III, the MC-FTN system model is presented and a continuous phase CP insertion scheme is introduced. Then, the FG-SS-BP equalization algorithm is extended to the MC-FTN system under the AWGN and multi-path fading channels. In Section IV, the complexity of the proposed equalization algorithm is analyzed. The simulation results are presented in Section V, whilst the conclusions are drawn in Section VI.

In this paper, lower case letters, lower case bold letters and upper case bold letters denote scalars, vectors and matrices respectively. x_k represents the kth element of vector $\mathbf{x}$. The superscript $(\cdot)^*$ denotes the conjugate. The symbols $|\cdot|$, $E\{\cdot\}$ and $\Re\{\cdot\}$ represent absolute value, expectation and real part operations. Furthermore, $a \propto b$ means that a is proportional to b.

II. The Proposed Algorithm for SC-FTN

A. SC-FTN System Model

In this section, we consider an SC-FTN system, the main blocks of which are shown in Fig. 1. At the transmitter, the information bits $\{c_k\}$ are coded by an LDPC encoder and then reordered by an interleaver. The information symbols $\{x_k\}$ are generated with the coded bits by an MPSK or MQAM modulator at the symbol rate $1/\tau T$, where $0 < \tau \leq 1$ is the compression factor. Then, the information symbols are passed through a T-orthogonal shaping filter $h(t)$ and transmitted over the channel. The transmitted SC-FTN signal $s(t)$ can be described by

$$s(t) = \sqrt{E_s} \sum_k x_k h(t - k\tau T),\ 0 < \tau \leq 1. \tag{1}$$

In this work, the root-raised-cosine (RRC) filter with roll-off factor α is used in order to reduce the length of the intrinsic ISI. For ISI-free transmission over an ideal AWGN channel of bandwidth W, the Nyquist orthogonal criterion must be satisfied which indicates $\tau = 1$. In an SC-FTN system, information symbols are transmitted at a higher rate, i.e., $\tau < 1$. Consequently, the channel capacity increases while the ISI is unavoidable.

At the receiver, the same pulse shape $h(t)$ is used as the matched filter. The received signal $y(t)$ is equalized iteratively and the FG-SS-BP equalizer outputs the soft information of the variables. Then, the soft output of the equalizer is used by the LDPC decoder to obtain the soft decoding information, which will be fed back to the equalizer as the outer layer a prior probability for the next turbo iteration. After several turbo iterations, the LDPC decoder will output the final decisions. In short, the proposed turbo scheme actually contains two layers of iterations. The inner iteration is the FG-SS-BP equalization and the outer iteration is the turbo iteration.

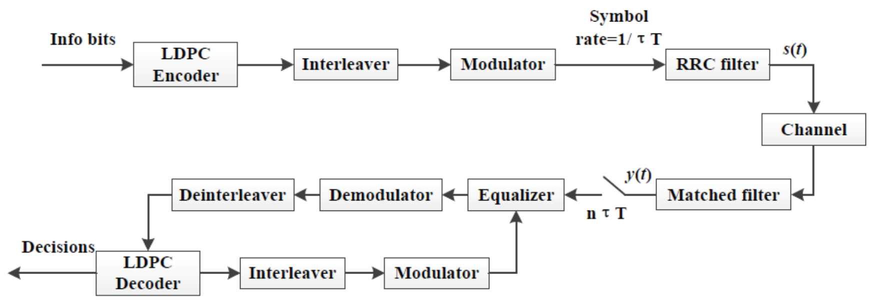

Fig. 1. SC-FTN system model

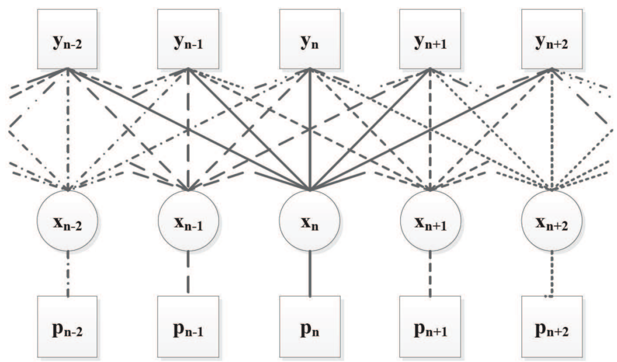

Fig. 2. Factor graph model of SC-FTN under the AWGN channel

Firstly, we introduce the FG-SS-BP equalization algorithm for the SC-FTN signaling under the AWGN channel. Then, the proposed algorithm is extended to a multi-path fading system model.

B. FG-SS-BP Equalization for SC-FTN Signaling under the AWGN Channel

The discrete-time SC-FTN system model can be written as

$$\mathbf{y} = \mathbf{G}\mathbf{x} + \mathbf{n}'. \tag{2}$$

In Eq. (2), $\mathbf{G} \in \mathbb{R}^{N\times N}$ is denoted by

$$\mathbf{G} = \begin{bmatrix} g_0 & \cdots & g_{-L} & 0 & 0 & \cdots & 0 \\ g_1 & g_0 & \cdots & g_{-L} & 0 & \cdots & 0 \\ \vdots & & \ddots & & & & \vdots \\ \vdots & & & \ddots & & & \vdots \\ \vdots & & & & \ddots & & \vdots \\ 0 & \cdots & 0 & g_L & \cdots & g_0 & g_{-1} \\ 0 & \cdots & \cdots & 0 & g_L & \cdots & g_0 \end{bmatrix}. \tag{3}$$

N is the number of symbols in an SC-FTN signal block and $g_l = g(l\tau T)$, where $g(t) = \int_{-\infty}^{\infty} h(\tau)h^*(\tau - t)d\tau$. $n'(t)$ is the colored Gaussian noise according to $n'(t) = \int_{-\infty}^{\infty} n(\tau)h^*(\tau - t)d\tau$, where $n(t)$ represents a Gaussian random variable with zero mean and two side power spectral density $\sigma_n^2/2$. The matrix $\mathbf{G}$ and the signal to noise ratio (SNR) are assumed to be perfectly known by the receiver in this paper. Thus, a posterior conditional probability function of the random vector $\mathbf{x}$, given $\mathbf{y}$ and $\mathbf{G}$ is

$$p(\mathbf{x}|\mathbf{G},\mathbf{y}) \propto \prod_{n=0}^{N-1} \exp(-\frac{1}{2\sigma^2}\eta_n^*\eta_n) \prod_{n=0}^{N-1} p_n(x_x), \tag{4}$$

where $\eta_n = y_n - \sum_{m=0}^{N-1} G_{n,m}x_m$ and $G_{n,m}$ denotes the entry on the nth row and mth column of the matrix $\mathbf{G}$. The FG model of the SC-FTN signaling under the AWGN channel is presented in Fig. 2. The transmitted symbols $x_i, 0 \le i \le N-1$ are variable nodes and the received symbols $y_i, 0 \le i \le N-1$ are treated as function nodes. Since each function node is only connected with several variable nodes, which are associated with it, the FG of the SC-FTN signaling is sparse. This can also be known from the sparse matrix $\mathbf{G}$ in Eq. (3). Then, the belief propagation (BP) algorithm can be applied to calculate marginal probability distribution of the transmitted variables.

In order to simplify the calculation, GA [20] is applied in the BP algorithm. According to Eq. (2) and (3), the received signal y_i can be rewritten as

$$y_i = \sqrt{E_s}x_l g_{i-l} + \sqrt{E_s}\sum_{\substack{j=i-v \\ j\neq l}}^{i+v} x_j g_{i-j} + n_i'. \tag{5}$$

$L_{ISI} = 2v$ is the number of the effective ISI taps. When y_i is used to estimate x_l, the second and the third items in Eq. (5) are considered to be the interference as a whole. Based on GA, the interference is modeled as

$$\sqrt{E_s}\sum_{\substack{j=i-v \\ j\neq l}}^{i+v} x_j g_{i-j} + n_i' \triangleq \delta_{il} \sim CN(\mu_{\delta_{il}}, \sigma_{\delta_{il}}^2). \tag{6}$$

The mean and variance of the interference are given by

$$\mu_{\delta_{il}} = \sqrt{E_s} \sum_{\substack{j=i-v \\ j\neq l}}^{i+v} g_{i-j} E(x_j), \tag{7}$$

$$\sigma^2_{\delta_{il}} = E_s \sum_{\substack{j=i-v \\ j\neq l}}^{i+v} |g_{i-j}|^2 Var(x_j) + \sigma^2_{n'}. \tag{8}$$

The conditional probability of the variable node x_l, calculated at y_i, is given by

$$p(x_l = \omega|\mathbf{G}, y_i) = \frac{1}{\sqrt{\pi\sigma^2_{\delta_{il}}}} \exp(-\frac{\|y_i - \mu_{\delta_{il}} - g_{i-l}\omega\|^2}{\sigma^2_{\delta_{il}}}), \tag{9}$$

where $\omega \in \mathcal{X}$ and $\mathcal{X}$ denotes the constellation set. The conditional probabilities computed at the function nodes are passed to the variable nodes. The variable nodes use them to calculate the probilities

$$p^i_{l,\omega} \triangleq p^i(x_l = \omega|\mathbf{y}) = \lambda^i_l \prod_{\substack{j=l-v \\ j\neq i}}^{l+v} p(x_l = \omega|\mathbf{G}, y_j), \tag{10}$$

$$\text{s. t.} \sum_{\omega\in\mathcal{X}} p^i_{l,\omega} = 1, \tag{11}$$

and then pass them back to the function nodes as a prior information for the next iteration. λ^i_l is chosen according to Eq. (11). After several iterations, the equalizer outputs the probabilities of the variables, which are given by

$$p(x_l = \omega) = \lambda_l \prod_{j=l-v}^{l+v} p(x_l = \omega|\mathbf{G}, y_j), \tag{12}$$

$$\text{s. t.} \sum_{\omega\in\mathcal{X}} p^i_{l,\omega} = 1, \tag{13}$$

In the proposed equalization algorithm, the serial-schedule (SS) updating mechanism is utilized. The updating procedure consists of forward recursion and backward recursion. The forward recursion, serially executed from x_0 to x_{N-1} is defined as

step 1: update the probabilities in (9) at all the function nodes connected with the virable node x_l and pass them to x_l;

step 2: update $p^i_{l,\omega}$ in (10) at x_l using the probabilities calculated in step 1 and pass them to the corresponding function nodes;

step 3: let $l = l + 1$ and go back to step 1.

Once the forward recursion is completed, the backward recursion is serially executed from x_{N-1} back to x_0, which will not be described in detail.

The iteration is terminated by setting a maximum iteration number. For an uncoded SC-FTN system, the outputs of the equalizer are used for making hard decisions on the transmitted data, i.e.,

$$\widehat{x_l} = \arg\max_{\omega \in \mathcal{X}} p(x_l = \omega), \tag{14}$$

while for the turbo scheme they are delivered to the LDPC decoder and used in the next turbo iteration.

C. Extension to the Multi-path Fading System Model

Consider a multi-path fading channel which can be modeled as a finite impulse response (FIR) filter with L_q taps, i.e., $\mathbf{q} = [q_0, q_1, \cdots, q_{L_q-1}]^T$. By defining

$$\overline{y}_i = \sqrt{E_s} \sum_{j=i-v}^{i+v} x_j g_{i-j}, \tag{15}$$

the received signal can be expressed as

$$\begin{aligned} y_i &= \sum_{m=0}^{L_q-1} q_m \overline{y}_{i-m} + n'_i \\ &= \sqrt{E_s} \sum_{m=0}^{L_q-1} \sum_{j=i-m-v}^{i-m+v} x_j q_m g_{i-m-j} + n'_i. \end{aligned} \tag{16}$$

The inter-dependencies among the variables of the SC-FTN signaling under a multi-path fading channel can also be represented by an FG model with more connections than that under a simple AWGN channel. For example, a single function node may be connected with as many as $L_{ISI} + L_q$ variable nodes when the delay spread spans over L_q symbol durations. Similar to the case under the AWGN channel, GA can be utilized in the SC-FTN system under multi-path fading channels and the FG-SS-BP equalization algorithm derived in Section II-B is also readily applicable in this multi-path scenario.

Note that the interference modeled by GA in the multi-path scenario is given by

$$\sqrt{E_s} \sum_{m=0}^{L_q-1} \sum_{\substack{j=i-m-v \\ j \neq l}}^{i-m+v} x_j q_m g_{i-m-j} + n'_i \triangleq \delta_{il} \sim CN(\mu_{\delta_{il}}, \sigma^2_{\delta_{il}}), \tag{17}$$

where the mean and variance of the interference are expressed as

$$\mu_{\delta_{il}} = \sqrt{E_s} \sum_{m=0}^{L_q-1} \sum_{\substack{j=i-m-v \\ j \neq l}}^{i-m+v} q_m g_{i-m-j} E(x_j), \tag{18}$$

$$\sigma^2_{\delta_{il}} = E_s \sum_{m=0}^{L_q-1} \sum_{\substack{j=i-m-v \\ j \neq l}}^{i-m+v} |q_m|^2 |g_{i-m-j}|^2 Var(x_j) + \sigma^2_{n'}. \tag{19}$$

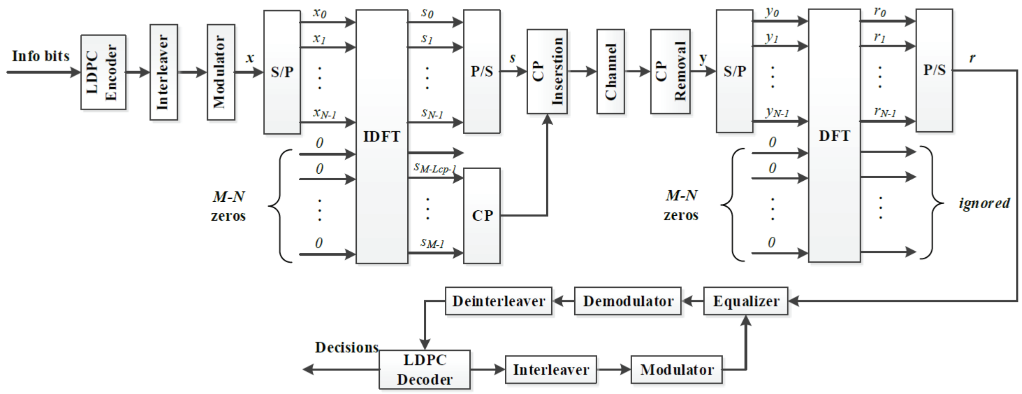

Fig. 3. MC-FTN system model

Hence, the probabilities of the variable node x_l, calculated at the function node y_i, can be written as

$$p(x_l = \omega|\mathbf{G}, y_i) = \frac{1}{\sqrt{\pi\sigma_{\delta_{il}}^2}} \exp(-\frac{\|y_i - \mu_{\delta_{il}} - \sum_{m=0}^{L_q-1} q_m g_{i-m-l}\omega\|^2}{\sigma_{\delta_{il}}^2}). \tag{20}$$

The procedure of the message passing is the same as that described in Section II-B.

III. The Proposed Equalization Algorithm for MC-FTN

A. MC-FTN System Model

In this section, we consider the MC-FTN system, where signals are stacked closer in frequency domain resulting in ISI. The frequency separation between the adjacent subcarriers is defined by

$$\Delta f = \frac{\phi}{T}, \ 0 < \phi \leq 1, \tag{21}$$

where ϕ is the compression factor. The MC-FTN signal $s(t)$ is given by

$$s(t) = \frac{1}{\sqrt{T}} \sum_{d} \sum_{n=0}^{N-1} x_{d,n} e^{j2\pi n \Delta f t}. \tag{22}$$

Here, $x_{d,n}$ denotes the information symbol modulated on the nth subcarrier of the dth MC-FTN symbol. N is the number of subcarriers of one MC-FTN symbol. When $\phi = 1$, $s(t)$ is the OFDM signal while when $\phi < 1$, it is the MC-FTN signal. Without loss of generality, we only consider the first MC-FTN symbol and the index d is therefore omitted. Hence, the transmitted signal, with a time window covering the first symbol period, is given by

$$s(t) = \frac{1}{\sqrt{T}} \sum_{n=0}^{N-1} x_n e^{j2\pi n \Delta f t}, \ 0 \leq t < T. \tag{23}$$

The discrete time representation of the system model, sampled every kT/N seconds, is written as

$$s_k = \frac{1}{\sqrt{N}} \sum_{n=0}^{N-1} x_n e^{\frac{j2\pi nk\phi}{N}}. \tag{24}$$

Assuming $\phi/N = 1/M$ and M is an integer, the MC-FTN signal can be generated by the IDFT framework proposed in [16]. The block diagram of the MC-FTN system is shown in Fig. 3.

At the transmitter, the elements of the modulated information sequence $\mathbf{x}$ are grouped by a serial to parallel converter and $M-N$ zeros are padded, i.e., $\widetilde{\mathbf{x}} = [x_0, x_1, \cdots, x_{N-1}, 0, \cdots, 0]^T$. M-point IDFT is carried out to generate the MC-FTN signal,

$$\widetilde{\mathbf{s}} = \mathbf{F}\widetilde{\mathbf{x}}. \tag{25}$$

Here, $\mathbf{F}$ is the $M \times M$ IFFT matrix with entries $f_{k,n} = \frac{1}{\sqrt{M}} e^{j2\pi nk/M}$. The first N elements of $\widetilde{\mathbf{s}}$ compose the transmitted MC-FTN symbol $\mathbf{s}$, i.e., $\mathbf{s} = [\widetilde{s}_0, \widetilde{s}_1, \cdots, \widetilde{s}_{N-1}]^T$. Then, an L_{CP}-length CP is inserted and the signal is transmitted over the channel.

In this work, a continuous phase CP insertion scheme is employed. For the conventional CP insertion scheme [16] of an OFDM system, the last L_{CP} items of the transmitted time domain sequence, i.e., $[\widetilde{s}_{N-L_{CP}}, \cdots, \widetilde{s}_{N-1}]$, are appended to the front of each OFDM symbol as the CP. However, in an MC-FTN system, the phase jump occurs if the same mechanism is applied. In order to suppress the out-band spurious spectrum caused by the phase discontinuity, we propose a continuous phase CP insertion scheme as

$$\mathbf{p} = [\widetilde{\mathbf{s}}_{M-L_{CP}}, \widetilde{\mathbf{s}}_{M-L_{CP}+1}, \cdots, \widetilde{\mathbf{s}}_{M-1}]^T. \tag{26}$$

As shown in Fig. 4, the phase between the CP and the MC-FTN symbol is continuous. In addition, the property of circular convolution is also satisfied in a multi-path fading scenario.

At the receiver, the CP is removed first and the received signal $\mathbf{y}$ is extended to length M by appending $M-N$ zeros such as $\widetilde{\mathbf{y}} = [\mathbf{y}^T, 0, \cdots, 0]^T$. $M \times M$ DFT is applied to transform $\widetilde{\mathbf{y}}$ to frequency domain signal $\widetilde{\mathbf{r}}$, which can be expressed as

$$\widetilde{\mathbf{r}} = \mathbf{F}^*\widetilde{\mathbf{y}}. \tag{27}$$

Then, $\widetilde{\mathbf{r}}$ is truncated to length N resulting in the vector $\mathbf{r} = [r_0, r_1, \cdots, r_{N-1}]^T$, which is subsequently used by the equalizer to estimate the transmitted signal $\mathbf{x}$.

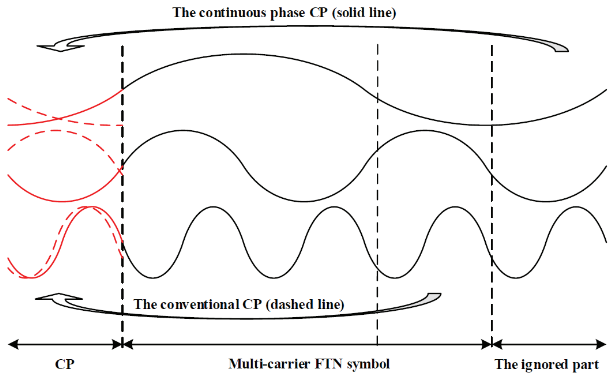

Fig. 4. The comparison of the continuous phase CP and the conventional CP for 3 different subcarriers

B. FG-SS-BP Equalization for MC-FTN under the AWGN Channel

Under AWGN assumptions, the extended received signal $\widetilde{\mathbf{y}}$ can be expressed as

$$\widetilde{\mathbf{y}} = \mathbf{I}_{M,N}\widetilde{\mathbf{s}} + \widetilde{\mathbf{n}}, \tag{28}$$

where $\mathbf{I}_{M,N} = \text{diag}(1, 1, \cdots, 1, 0, \cdots, 0)$ is a diagonal matrix, with the first N diagonal values 1 and the rest diagonal values 0. $\widetilde{\mathbf{n}} = [n_0, n_1, \cdots, n_{N-1}, 0, \cdots, 0]^T$ is a vector of length M, whose first N elements are Gaussian variables with zero mean and two sided power spectral density $\sigma_n^2/2$, and the last $M-N$ elements are zeros. After demodulated by the DFT, the reception process can be expressed as

$$\widetilde{\mathbf{r}} = \mathbf{F}^*\widetilde{\mathbf{y}} = \mathbf{F}^*\mathbf{I}_{M,N}\mathbf{F}\widetilde{\mathbf{x}} + \widetilde{\mathbf{n}}_{\mathbf{F}^*}, \tag{29}$$

where $\widetilde{\mathbf{n}}_{\mathbf{F}^*} = \mathbf{F}^*\widetilde{\mathbf{n}}$. Since $\mathbf{I}_{M,N}$ is not an identity matrix, the production of $\mathbf{F}^*\mathbf{I}_{M,N}\mathbf{F}$ is not a diagonal matrix. As a result, the ICI is introduced.

Let us denote

$$\widetilde{\mathbf{G}} = \mathbf{F}^*\mathbf{I}_{M,N}\mathbf{F} = [G_{m,n}],\ 0 \leq m, n \leq M-1, \tag{30}$$

where $G_{m,n}$ are the entries of $\widetilde{\mathbf{G}}$. Define $\mathbf{G}' \in \mathbb{C}^{N\times N}$ to be the submatrix of $\widetilde{\mathbf{G}}$, which is composed of

$G_{m,n}, 0 \leq m, n \leq N-1$ such as

$$\widetilde{\mathbf{G}} = \begin{bmatrix} & & & G_{0,N} & \cdots & G_{0,M\text{-}1} \\ & \mathbf{G}' & & \vdots & & \vdots \\ & & & G_{N\text{-}1,N} & \cdots & G_{N\text{-}1,M\text{-}1} \\ G_{N,0} & \cdots & G_{N,N\text{-}1} & G_{N,N} & \cdots & G_{N,M\text{-}1} \\ \vdots & & \vdots & \vdots & & \vdots \\ G_{M\text{-}1,0} & \cdots & G_{M\text{-}1,N\text{-}1} & G_{M\text{-}1,N} & & G_{M\text{-}1,M\text{-}1} \end{bmatrix}. \tag{31}$$

By eliminating the useless parts, Eq. (31) can be simplified as

$$\mathbf{r} = \mathbf{G}'\mathbf{x} + \mathbf{n}_{\mathbf{F}^*}, \tag{32}$$

where $\mathbf{r}$ and $\mathbf{n}_{\mathbf{F}^*}$ are composed of the first N elements of $\widetilde{\mathbf{r}}$ and $\widetilde{\mathbf{n}}_{\mathbf{F}^*}$, respectively. The elements of $\mathbf{r}$ can be written as

$$r_m = \frac{1}{M} \sum_{n=0}^{N-1} x_n \sum_{k=0}^{N-1} e^{\frac{j2\pi(n-m)k}{M}} + \widetilde{n}_{\mathbf{F}^* m}. \tag{33}$$

An MC-FTN symbol can be essentially viewed as an OFDM symbol truncated by a rectangular window. The duration of the rectangular window is T seconds while the OFDM symbol has the duration MT/N seconds. The subcarriers are located at the non-zero points of the sinc function, which is the Fourier transform of the rectangular window, the ICI is thus produced. The FG-SS-BP equalization algorithm is also applicable to MC-FTN systems. However, the sinc function generates more ICI taps than the RRC filter does, which is used in the SC-FTN signaling in Section II. When $\tau = \phi = 0.8$, the amplitudes of the RRC filter taps with $\alpha = 0.3$ need $v = 3$ to decrease below 5% of the maximum value, while $v = 7$ is needed for the sinc filter. For a large scale MC-FTN system under the AWGN channel, the number of the effective ICI taps can also be truncated to $L_{ISI} = 2v$ to reduce the complexity.

C. Extension to the Multi-path Fading System Model

The MC-FTN system model under the multi-path fading channel can be expressed as

$$\widetilde{\mathbf{r}} = \mathbf{F}^* \mathbf{I}_{M,N} \mathbf{Q} \mathbf{I}'_{M,N} \mathbf{F} \widetilde{\mathbf{x}} + \widetilde{\mathbf{n}}_{\mathbf{F}^*}. \tag{34}$$

Here, $\mathbf{Q}$ is a circulation matrix, which is defined by

$$\mathbf{Q}=\begin{bmatrix} q_0 & 0 & \cdots & 0 & q_{L_q-1} & \cdots & q_2 & q_1 \\ q_1 & q_0 & 0 & \cdots & 0 & q_{L_q-1} & \cdots & q_2 \\ \vdots & & & \vdots & & & \vdots & \\ q_{L_q-1} & \cdots & q_2 & q_1 & q_0 & 0 & \cdots & 0 \\ \vdots & & & \vdots & & & & \vdots \\ 0 & \cdots & 0 & q_{L_q-1} & q_{L_q-2} & \cdots & q_1 & q_0 \end{bmatrix}, \tag{35}$$

where $\mathbf{q}=[q_0,q_1,\cdots,q_{L_q-1}]^T$ is the channel impulse response with L_q taps. The matrix $\mathbf{I}'_{M,N}$ is a diagonal matrix with the diagonal values such as

$$I_{m,m}=\begin{cases} 1 & 0\le m\le N-1 \\ 0 & N\le m\le M-L_q-1 \\ 1 & M-L_q\le m\le M-1 \end{cases}. \tag{36}$$

In order to establish the FG model, the first N elements of the DFT output vector $\widetilde{\mathbf{r}}$ can be written as

$$r_m=\frac{1}{M}\sum_{n=0}^{N-1}x_n\sum_{l=0}^{L_q-1}q_l\sum_{k=0}^{N-1}e^{\frac{j2\pi(nk-nl-mk)}{M}}+\widetilde{n}_{\mathbf{F}^*m}. \tag{37}$$

Consequently, the parameters on each edge connecting variable nodes and function nodes can be determined. Since the multi-path fading affects the entire spectrum, the FG of the MC-FTN system under multi-path fading channels is a full-connection FG.

IV. Complexity Analysis

We first consider the complexity of the proposed equalization algorithm in an SC-FTN system under the AWGN channel. According to Section II-B, we know that the procedure of the backward recursion is almost the same as that of the forward recursion. Hence, only the complexity of the forward recursion is analyzed. The complexity in terms of multiplications, additions and exponents of the main steps of the forward recursion is shown in Table I, where K is the modulation order. For example, when 16QAM is considered, K is 4. By summing the complexity in Table I, the complexity of message passing for a single variable node is in the order of $O(2^{K/2+1}L_{ISI})$. Considering the length of the FTN signal block, the total complexity of the FG-SS-BP equalization algorithm is $O(2^{K/2+1}NL_{ISI})$. For comparison, the complexity of SOTMVA [5] is $O(2^{KL_{ISI}}N)$, which is much higher than the proposed algorithm, and TMVA needs almost the same complexity.

TABLE I

COMPLEXITY OF THE MAIN STEPS OF THE PROPOSED ALGORITHM

Step	Multiplications	Additions	Exponents
$\mu_{\delta_{il}}$ in Eq. (7)	$2^{K/2+1}L_{ISI} + L_{ISI} + 1$	$2^{K/2+1}L_{ISI} - 1$	0
$\sigma^2_{\delta_{il}}$ in Eq. (8)	$2^{K/2+1}L_{ISI} + L_{ISI} + 3$	$2^{K/2+1}L_{ISI} + L_{ISI}$	0
$p(x_l = \omega \vert \mathbf{G}, y_i)$ in Eq. (9)	$4 \cdot 2^{K/2+1}$	$2 \cdot 2^{K/2+1}$	$2^{K/2+1}$
$p^i_{l,\omega}$ in Eq. (10)	$2^{K/2+1}L_{ISI}$	$2^{K/2+1} - 2$	0

When the proposed algorithm is applied to the SC-FTN system under multi-path fading channels, a single function node may be connected with as many as $L_{ISI} + L_q$ variable nodes in the FG as mentioned in Section II-C. Calculated in a similar way, the complexity of the the proposed algorithm for SC-FTN under multi-path fading channels is in the order of $O(2^{K/2+1}N(L_{ISI} + L_q))$.

Similarly, the complexity of the proposed FG-SS-BP equalization algorithm for MC-FTN systems can be analyzed. The complexity of the proposed algorithm for MC-FTN under the AWGN channel is $O(2^{K/2+1}NL_{ICI})$ due to the truncation, where N is the number of subcarriers in a single MC-FTN symbol and L_{ICI} is the number of effective ICI taps. For comparison, the complexity of the ID-FSD detection algorithm under the AWGN channel in [14] is $O(2^{K/2+1}N^2) + O(T_wKN)$, where T_w is the value of tree width. The proposed algorithm needs much less complexity than the ID-FSD algorithm. As to the MC-FTN under multi-path fading channels, the algorithm needs the complexity of $O(2^{K/2+1}N^2)$ for the FG is a full-connection FG.

V. SIMULATION RESULTS

A. Simulation Results of SC-FTN Signaling

The BER performance comparison of the proposed algorithm with some exiting algorithms in an uncoded SC-FTN system under the AWGN channel is shown in Fig. 5. α and τ are set to be 0.1 and 0.9, and QPSK modulation is employed for simplicity. According to Fig. 5, the performance of SOTMVA-RISIC is nearly the same as the optimal detector under ISI-free conditions. TMVA performs worse than SOTMVA-RISIC. The reason is that SOTMVA-RISIC not only uses the soft information but also introduces an RISIC, which is not adopted in TMVA. The proposed FG-SS-BP algorithm performs very close to SOTMVA-RISIC as well as the ISI-free benchmark, with a gap of about 0.2dB at 10^{-3}. However, it has much lower complexity than SOTMVA-RISIC.

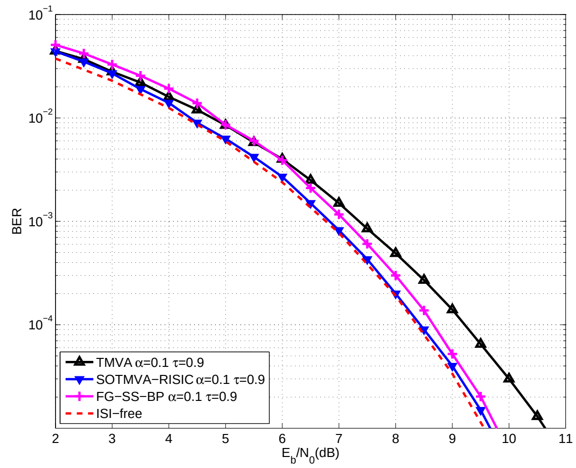

Fig. 5. BER performance comparison in an uncoded SC-FTN system with $\alpha = 0.1$, $\tau = 0.9$

Fig. 6 shows the BER performance of the proposed algorithm under the AWGN and the SUI3 channel with $\alpha = 0.3$. When QPSK modulation is employed, the performance of the proposed algorithm under the AWGN channel with $\tau = 0.9$ is nearly the same with the ISI-free benchmark. The gap between these two curves is smaller than that between the performance with $\alpha = 0.1,\ \tau = 0.9$ and the benchmark as shown in Fig. 5. The reason is that the ISI caused by the RRC filter with $\alpha = 0.1$ is more severe than that with $\alpha = 0.3$. The performance with $\tau = 0.8$ is slightly worse than benchmark, while 25% increase in data rate can be achieved. Apparently, the ISI introduced by SC-FTN signaling becomes more serious when τ decreases. Simulated under the SUI3 channel, the performance of the proposed algorithm with $\tau = 0.9$ is close to the performance under the AWGN channel. When $\tau = 0.8$, performance gap between the AWGN and SUI3 channels increases to about 1dB at 10^{-3}. It is because the ISI is much fiercer with a lower τ in multi-path fading channels. When 16QAM modulation is employed, the performance under the AWGN channel with $\tau = 0.9$ and $\tau = 0.85$ is close to the optimal detector of a 16QAM orthogonal system, while the performance suffers from a 1dB degradation at 10^{-3} when simulated under the SUI3 channel with $\tau = 0.9$, and the gap increases to 2dB when τ decreases to 0.85. The simulation results demonstrate that the proposed algorithm is robust against the intrinsic ISI and multi-path fading in an SC-FTN system with high-order modulation, especially when τ is large.

Fig. 7 shows the performance of the turbo detection based on the FG-SS-BP equalization algorithm. The LDPC code with code rate $1/2$ is employed. The turbo iteration number is $\{1, 3, 5\}$. α and τ are set to 0.3 and 0.9, respectively. It can be seen from Fig. 7 that the performance of the turbo detection

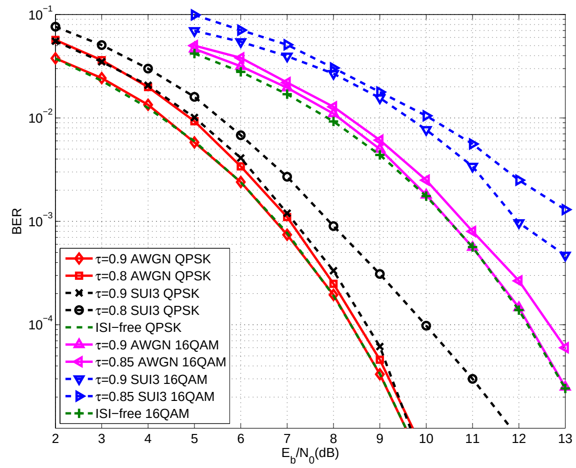

Fig. 6. BER performance in an uncoded SC-FTN system with $\alpha = 0.3$

scheme under the AWGN channel is close to the ISI-free benchmark. The performance is improved when increasing the turbo iteration number. There is some performance degradation when the proposed turbo detection scheme is applied to the SC-FTN system under the SUI3 channel, compared to the AWGN channel. A gap of about 1.1dB is found at 10^{-6} between the BER curves of the AWGN and SUI3 channels with QPSK modulation when the iteration number is 5. With 16QAM, the gap is about 1.2dB. The reason is that the SUI3 channel causes extra ISI on the basis of the intrinsic ISI introduced by the SC-FTN signaling.

B. Simulation Results of MC-FTN Signaling

Fig. 8 (a) and (b) shows the BER performance of the FG-SS-BP equalization algorithm for an uncoded MC-FTN system as well as the performance of the turbo detection, respectively. In all simulations, the continuous phase CP insertion scheme is employed and the number of the subcarriers of one symbol is set to $N = 32$. The performance of the OFDM with N subcarriers is also presented for comparison.

In the uncoded MC-FTN system, the performance of the proposed algorithm is slightly worse than the performance of OFDM under the AWGN channel. When QPSK is employed and $\phi = 0.8$, there is a gap of about 1dB at 10^{-3} and 0.25dB at 10^{-5}. As E_b/N_0 increases, the gap between the two curves becomes smaller. The reason is that the transmitted symbols can be equalized more accurately when the E_b/N_0 is high enough. For comparison, the performance of the ID-FSD algorithm in [14] is also presented. It can be seen that the proposed algorithm outperforms the ID-FSD algorithm when E_b/N_0 is above 9dB

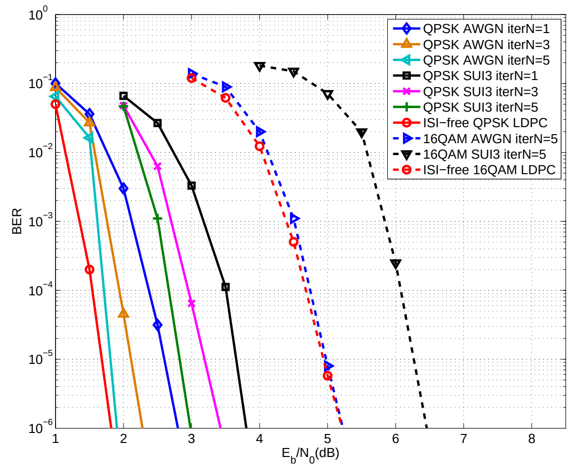

Fig. 7. BER performance of turbo detection for SC-FTN with $\alpha = 0.3$ and $\tau = 0.9$

and the gap is potential to increase with E_b/N_0. In the meanwhile, the proposed algorithm needs less complexity than ID-FSD as analyzed in Section IV. In the case of 16QAM-modulated MC-FTN with $\phi = 0.94$, which is chosen to ensure M is an integer, the performance of the proposed algorithm is pretty close to the performance of OFDM when E_b/N_0 is lower than 11dB. When E_b/N_0 goes beyond 11dB, the BER curve declines more slowly since the intrinsic ICI becomes dominant. The proposed algorithm cannot eliminate completely the ICI due to the complex constellation of 16QAM. However, the performance penalty can be compensated by turbo detection.

When we consider the turbo detection scheme, the performance of the coded OFDM is presented as the benchmark. Since there is no ICI in OFDM under both the AWGN and SUI3 channels, the equalizer and turbo structure are not applied in the OFDM system while only a pair of LDPC encoder and decoder is used. The maximum number of turbo iterations is set to 5. According to Fig. 8 (b), the BER curves fall sharply when turbo detection is applied. When QPSK modulation is applied, the performance with $\phi = 0.8$ is merely 0.8dB worse than the benchmark at 10^{-6} under the AWGN channel, while a same gap is found under the SUI3 channel. The performance degradation under the SUI3 channel, compared to the AWGN channel, is reasonable because the SUI3 channel leads to deep fade at some subcarriers. Considering 16QAM, the performance with $\phi = 0.94$ under the AWGN channel is almost optimal at 10^{-6} and it suffers from a 0.5dB degradation under the SUI3 channel. When ϕ decreases to 0.88, the gaps between the benchmark and the performance under the AWGN channel, as well as the SUI3 channel, are both 1.2dB. The simulation results demonstrate that the turbo detection can improve the performance significantly and a portion of bandwidth can be saved. For example, 20% bandwidth is saved when $\phi = 0.8$. The improved bandwidth efficiency makes MC-FTN a viable and appealing solution, despite the extra complexity incurred in the equalization process.

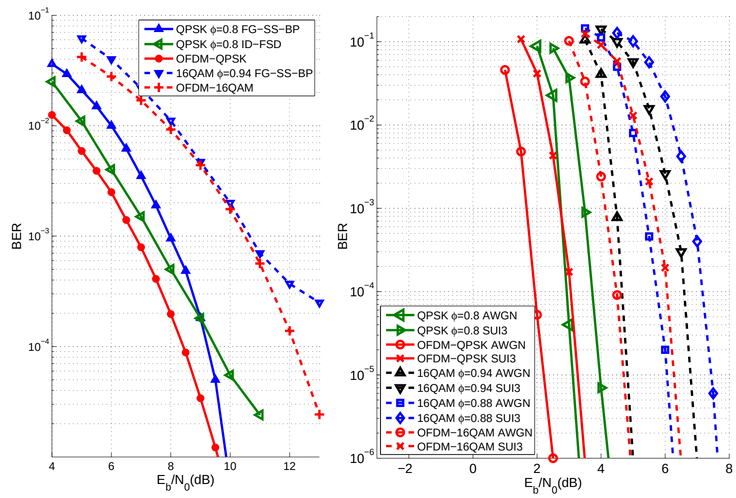

(a) BER performance in an uncoded MC−FTN system

(b) BER peformance of the turbo detection

Fig. 8. BER performance of the proposed algorithm for MC-FTN with $N = 32$

VI. Conclusion

Motivated by the advantages of the FTN concept as well as the drawbacks of the intrinsic ISI and ICI, we have proposed a low-complexity turbo detection scheme based on the FG-SS-BP equalization algorithm for SC-FTN and MC-FTN signaling with high-order modulation, such as MPSK and MQAM. In this paper, AWGN and multi-path fading channels are both considered. In order to reduce the complexity, GA is applied to the proposed algorithm. Furthermore, a continuous phase CP insertion scheme is proposed to maintain the properties of continuous phase and circular convolution. The simulation results demonstrate that the proposed low-complexity equalization algorithm achieves near-optimum performance with up to 20% time or bandwidth saving. In addition, turbo detection can further improve the performance of the system. However, the complexity of the proposed algorithm for MC-FTN under multi-path fading channels needs to be further reduced. Ongoing work includes the reduced-complexity scheme for MC-FTN signaling under multi-path fading channels based on a proper truncation principle to maintain the sparse nature of the FG. In summary, the FG-SS-BP equalization algorithm is an applicable and promising technique for SC-FTN and MC-FTN signaling for 5G mobile communications.

References

[1] James, E.M.: ‘Faster-than-Nyquist signaling’, Bell Syst. Tech. J., 1975, 54, (8), pp. 1451-1462

[2] Fredrik, R., John, B.A.: ‘Constrained capacities for faster-than-Nyquist signaling’, IEEE Trans. Inform. Theory, 2009, 55, (2), pp. 764-775

[3] John, B.A., Fredrik, R., Viktor, O.: ‘Faster than Nyquist signaling’, Proc. IEEE, 2013, 101, (8), pp. 1817-1830

[4] G., D.F.: ‘Maximum-likelihood sequence estimation of digital sequences in the presence of intersymbol interference’, IEEE Trans. Inform. Theory, 1972, 18, (3), pp. 363-378

[5] Angelos, D.L., Costas, N.G.: ‘Exploiting faster-than-Nyquist signaling’, IEEE Trans. on Commun., 2003, 51, (9), pp. 1502-1511

[6] Adnan, P., John, B.A.: ‘Reduced-complexity receivers for strongly narrowband intersymbol interference introduced by faster-than-Nyquist signaling’, IEEE Trans. Commun., 2012, 60, (9), pp. 2591-2601

[7] Shinya, S.: ‘Frequency-domain equalization of faster-than-Nyquist signaling’, IEEE Commun. Lett., 2013, 2, (5), pp. 1-4

[8] Shinya, S., Lajos, H.: ‘Frequency-domain equalization aided iterative detection of faster-than-Nyquist signaling’, IEEE Trans. Veh. Technol., 2015, 64, (5), pp. 2122-2128

[9] Fredrik, R., John, B.A.: ‘Multistream faster-than-Nyquist signaling’, IEEE Trans. Commun., 2009, 57, (5),pp. 1329-1340

[10] Alan, B., Dario, F., Giulio, C.: ‘Time-frequency packing for linear modulation: spectral efficiency and practical detection schemes’, IEEE Trans. Commun., 2009, 57, (10), pp. 2951-2959

[11] Ioannis, K.: ‘Spectrally efficient multicarrier communication systems: Signal detection, mathematical modelling and optimisation,” PhD. dissertation, University College London, 2010.

[12] Safa, I., Izzat, D.: ‘Precoded spectrally efficient FDM system’. Proc. IEEE Conf. Pers. Indoor Mobile Radio Commun., Istanbul, Turkey, Sep. 2010, pp. 99-104

[13] Ioannis, K., Arsenia, C., Miguel, R.D., R., Izzat, D.: ‘Spectrally efficient FDM signals: bandwidth gain at the expense of receiver complexity’. Proc. IEEE Int. Conf. on Commun., Dresden, Germany, Jun. 2009, pp. 1-6

[14] Tongyang, X., Ryan, C.G., Farokh, M., Izzat, D.: ‘An improved fixed sphere decoder employing soft decision for the detection of non-orthogonal signals’, IEEE Commun. Lett., 2013, 17, (10), pp. 1964-1967

[15] Tongyang, X., Izzat, D.: ‘Spectrally efficient FDM: spectrum saving technique for 5G?’ Proc. IEEE Int. Conf. on 5GU, Akaslompolo, Finland, Nov. 2014, pp. 273-278

[16] Safa, I., Izzat, D.: ‘Simple DSP-IDFT techniques for generating spectrally efficient FDM signals’. Proc. IEEE IET Int. Symp. Commun. Syst. Netw. Digital Signal Process., Newcastle, UK, Jul. 2010, pp. 20-24

[17] Paul, N.W., Marcus, R.P., Safa, I., Izzat, D.: ‘VLSI architecture for a reconfigurable spectrally efficient FDM baseband transmitter’, IEEE Trans. on Circuit and Syst., 2012, 59, (6), pp, 1107-1118

[18] Tongyang, X., Izzat, D.: ‘Multi-band reduced complexity spectrally efficient FDM systems’. Proc. IEEE IET Int. Symp. Commun. Syst., Netw. Digital Signal Process., Manchester, UK, Jul. 2014, pp. 982-987

[19] Tianhang, Y., Minjian, Z., Jie, Z., Yunlong, C.: ‘Low-Complexity Detection for FTN Signaling Based on Weighted FG-SS-BP Equalization Method’. Proc. IEEE Veh. Technol. Conf., Nanjing, China, May 2016, pp. 1-5

[20] Xiaomu, Z., Yabo, L., Jie, Z., Minjian, Z., Chen, Z.: ‘Low-complexity layered joint detection and decoding for LDPC coded large-MIMO systems’. Proc. IEEE Int. Conf. Wirel. Commun. Signal Precess., Hangzhou, China, Oct. 2013, pp. 1-6

[21] Giulio, C., Dario, F., Amina, P.: ‘SISO detection over linear channels with linear complexity in the number of interferers’, IEEE J. Sel. Topics Signal Process., 2011, 5, (8), pp. 1475-1485